Journal of Optoelectronics and Advanced Materials Vol. 5, No. 5, 2003, p. 1169 - 1179

POST-IRRADIATION THERMALLY STIMULATED RECOVERING OF SOME TERNARY CHALCOGENIDE GLASSES

O. Shpotyuk[a,b*], A. Kovalskiy[a,c], T. Kavetskyy[a], R. Golovchak[a]

[a]Scientific Research Company "Carat", Stryjska str. 202, 79031 Lviv, Ukraine
[b]Physics Institute, Pedagogical University, Al. Armii Krajowej 13/15, 42201 Czestochowa, Poland
[c]Institute for Telecommunications, Radioelectronics and Electronic Engineering, National University "Lviv Polytechnics", Bandera str. 12, 79013 Lviv, Ukraine

The influence of thermal annealing temperature T_a on the radiation-induced optical effects' (RIOEs) control parameter $\chi(h\nu)=\Delta\alpha/\alpha_0(h\nu)$ (where α_0 and α are respectively the values of optical absorption coefficient before and 3 months after the γ-irradiation, $h\nu$ is the photon energy) is studied for some chalcogenide glasses of As–Sb–S, Ge–As–S and Ge–Sb–S ternary systems on pseudobinary 'stiochiometric' As_2S_3–Sb_2S_3, As_2S_3–GeS_2, Sb_2S_3–GeS_2 and 'non-stoichiometric' As_2S_3–Ge_2S_3, Sb_2S_3–Ge_2S_3 cut-sections. The compositional features of the apparent activation energies obtained from different ranges of $\ln\chi=f(10^3/T_a)$ dependence are analyzed. Interpretation of the form of $\ln\chi=f(10^3/T_a)$ curve in various T_a regions is given for the first time in detail. Possible mechanisms of the observed post-irradiation thermally stimulated restoration (ThSR) effects are also considered.

(Received July 9, 2003; accepted August 28, 2003)

Keywords: Chalcogenide glasses, Thermal annealing, γ-irradiation, Optical properties

1. Introduction

Chalcogenide glasses (ChG) remain interesting objects in physics of disordered solids due to their potential application in optoelectronics as optical wavequides, optical gratings, IR sensors, etc. [1-3]. In this connection, apparently, the research of influence of external factors on the physical properties of these materials is a very important problem. Recently, we have considered the peculiarities of the radiation-induced optical effects (RIOE) stimulated by Co^{60} γ-quanta with energy more than 1 MeV in some ternary ChG, such as As–Sb–S, Ge–As–S and Ge–Sb–S systems [4]. It is significant that γ-irradiation causes the 'red' shift of the fundamental optical absorption edge (γ-induced 'darkening' effect) for ChG of these systems and it essentially depends on the glass chemical composition. Similar features of induced phenomena have been determined in the case of photoexposure of ChG too [5]. Moreover, the both photo- and γ-induced changes of optical properties are reversible in cycle of irradiation and annealing at the temperature close to glass transition temperature T_g [4,5]. In the case of photoexposure, the reversible properties are widely used for optical recording and storage of information [6], while, in the case of γ-irradiation, the reversible properties can be explored in creation of γ-irradiation sensors.

However, the dependence of γ-induced phenomena on the thermal annealing temperature T_a up to near T_g has not been studied yet in detail. For example, we have partially considered such processes for preliminarily γ-irradiated vitreous v-As_2S_3 binary and v-As–Sb–S ternary ChG [7,8]. Namely, some features of apparent activation energy obtained from $\ln\chi=f(10^3/T_a)$ curve (where χ stands for the RIOEs' control parameter) have been only discussed for these ChG, whereas the

* Corresponding author: shpotyuk@novas.com.ua

analysis of the curve form has not been carried out. The latter is a very interesting, especially taking into account that the form of $\ln\chi=f(10^3/T_a)$ curve differs in various T_a regions.

Thus, the aim of the present article is to investigate in detail the dependence of the RIOE control parameter on the annealing temperature for ternary As–Sb–S, Ge–As–S and Ge–Sb–S ChG along pseudobinary 'stoichiometric' and 'non-stoichiometric' cut-sections.

2. Experimental

The bulk samples from pseudobinary 'stiochiometric' As_2S_3–Sb_2S_3, As_2S_3–GeS_2, Sb_2S_3–GeS_2 and 'non-stoichiometric' As_2S_3–Ge_2S_3, Sb_2S_3–Ge_2S_3 cut-sections of As–Sb–S, Ge–As–S and Ge–Sb–S ternary systems with different values of average coordination number Z (number of covalent chemical bonds per atom of glass formula unit) were chosen for investigations (Table 1). The Z values have been obtained according to formula [9]:

$$Z = \Sigma n_m m/\Sigma n_m, \quad (1)$$

where n_m is a number of atoms with m coordination.

So, in the case of $Ge_xSb(As)_ySz$ ternaries the Z values can be calculated as follows:

$$Z = (4x + 3y + 2z)/(x + y + z), \quad (2)$$

where 4, 3, and 2 stand for coordination numbers of Ge, Sb(As) and S atoms, respectively.

Table 1. The values of average coordination number Z, glass transition temperature T_g (taken from Refs. given in square brackets), maximal restoration temperature and apparent activation energies E_a and E_{AB} of post-irradiation thermally stimulated restoration effects (determined experimentally from $\ln\chi_{max} = f(10^3/T_a)$ dependences) for investigated glass compositions of ternary As–Sb–S, Ge–As–S and Ge–Sb–S systems. Detailed explanation of T_{max}, E_a and E_{AB} parameters is given in the text of the article.

ChG compositions	Z	T_g (K)	T_{max} (K)	E_a (eV)	$-E_{AB}$ (eV)
$As_{40}S_{60}$	2.40	465±5 [10]	455	0.27±0.02	0.009
$As_{28}Sb_{12}S_{60}$	2.40	470±5 [10]	435	0.10±0.02	0.011
$Ge_{4.3}As_{34.8}S_{60.9}$	2.43	485 [10]		0.07±0.02	0.026
$Ge_{9.5}As_{28.6}S_{61.9}$	2.48	515 [10]		0.11±0.02	0.018
$Ge_{15.8}As_{21}S_{63.2}$	2.53	555 [10]		0.12±0.02	0.006
$Ge_{23.5}As_{11.8}S_{64.7}$	2.59	618 [10]		0.13±0.02	0.021
$Ge_{23.5}Sb_{11.8}S_{64.7}$	2.59	685 [11]	560	0.22±0.02	0.013
$Ge_{28.125}Sb_{6.25}S_{65.625}$	2.63	718 [11]	560	0.24±0.02	0.015
$Ge_{16}As_{24}S_{60}$	2.56	530 [10]		0.18±0.02	0
$Ge_{24}As_{16}S_{60}$	2.64	620 [10]		0.51±0.05	0
$Ge_{32}As_8S_{60}$	2.72	670-675 [10]		0.62±0.05	0
$Ge_{36}As_4S_{60}$	2.76	682 [10]	540	0.10±0.02	0
$Ge_{27}Sb_{13}S_{60}$	2.67	603 [12]		0.20±0.02	0.035
$Ge_{35}Sb_5S_{60}$	2.75	643 [12]		0.20±0.02	0.040

The investigated samples were prepared by a melt-quenching method [12] using the mixture of high purity (99,9999%) Ge, Sb, As and S, sealed in quartz ampoules (10^{-3} Pa) and heated gradually up to 1200 K. The furnace was rocked for 24 hours in order to obtain the most homogeneous melt. Then the obtained ingots were quenched in air at T=290 K. All ampoules were annealed additionally at the temperature of 20-30 K below softening point T_g to remove the appeared mechanical strains. The amorphous state of the investigated materials was controlled by characteristic conchoidal fracture, data of X-ray diffraction analysis and IR microscopy. Finally, all ingots have been sliced into disks of 1-2 mm thickness and polished for optical measurements.

The ChG samples were irradiated with γ-quanta at the normal conditions of stationary radiation field, created in the closed cylindrical cavity owing to concentrically established ^{60}Co (E=1.25 MeV) sources [4]. No special procedures were used to prevent the uncontrolled thermal annealing of the samples, but the maximal temperature in the irradiating camera did not exceed 320-330 K during whole period of irradiation. The optimal accumulated doses (in the range 2.2÷10 MGy) were chosen for investigated ChG, taking into account the previous researches of radiation-induced phenomena in amorphous chalcogenides [7].

Double-beam spectrophotometer "Specord M-40" (200-900 nm) was used for transmission measurements of investigated ChG before and after γ-irradiation. The special marks were drawn on the sample surfaces to avoid the measurement errors connected with sample position in device camera. Accuracy of the measurement was ±0.5%.

T_a influence on the optical transmittance spectra of the preliminarily γ-irradiated ChG was studied in the temperature range from T=290 K up to near T_g with step 20-30 K using a high-temperature camera HPS-222 (“Tabai”). Time of heating of the investigated ChG in the camera was 30 min for each T_a value. The temperature in the camera was controlled with the accuracy ± 1 K. After annealing the samples were quenched on air at T=290 K during 30 min before every optical transmission measurement.

The spectral dependence of the optical absorption coefficient differences $\Delta\alpha/\alpha_0(h\nu)=\chi(h\nu)$ (α_0 and α are the values of optical absorption coefficient before and 3 months after γ-irradiation, respectively; $h\nu$ is the photon energy) was chosen as the controlled parameter for the RIOE. The α values are calculated from the well-known formula [13]:

$$\alpha = 1/d \ln((1 - r)^2/\tau), \tag{3}$$

where d, r and τ are the thickness, coefficient of reflection and transmission of samples, respectively.

3. Results

Fig. 1 shows the spectral dependence of relative γ-induced changes (Φ=3 MGy) in the optical absorption coefficient $\Delta\alpha/\alpha_0$ on the photon energy $h\nu$ at different temperatures by the example of ChG chemical composition $Ge_{28.125}Sb_{6.25}S_{65.625}$ with value of the average coordination number Z=2.63 from the pseudobinary ‘stoichiometric’ Sb_2S_3-GeS_2 cut-section of Ge–Sb–S system. In this figure the obtained data at room temperature (T=290 K) correlate with the γ-induced optical changes before thermal influence (i.e. the post-irradiation RIOE). Others experimental data demonstrate the effect of the annealing temperature T_a on the observed γ-induced optical changes.

It can be seen the additional ‘darkening’ effect at low annealing temperatures (arrow up in the T_a≅313-373 K region, Fig. 1), which is represented by $\Delta\alpha/\alpha_0(h\nu)$ curves above the initial $\Delta\alpha/\alpha_0(h\nu)$ curve (at T=290 K, Fig. 1), which belongs to γ-induced state before thermal annealing.

When the thermal annealing temperature is greater than T_a=373 K, the γ-induced optical effect decreases or the post-irradiation thermally stimulated restoration (ThSR) effect is observed. Apparently, this ThSR phenomenon increases with annealing temperature (arrow down, Fig. 1).

At the very high temperatures (close to T_g), some increase of the γ-induced optical effect is observed (arrow up in the T_a≅563-653 K region, Fig. 1).

Thus, we can distinguish three T_a regions (the low-temperature region, the threshold temperature region and the high-temperature region) where the different behavior of γ-induced darkening effect as a function of annealing temperature takes place.

By taking advantage of description of the γ-induced optical effect through $\chi_{max}=(\Delta\alpha/\alpha_0)_{max}$ parameter (the maximal value of the relative change of optical absorption coefficient α, Fig. 1), the observed thermally-induced changes in RIOE in the investigated ChG systems can be adequately interpreted using χ_{max} parameter, which being a function of the thermal annealing temperature T_a possesses an activation character with apparent activation energies E_a.

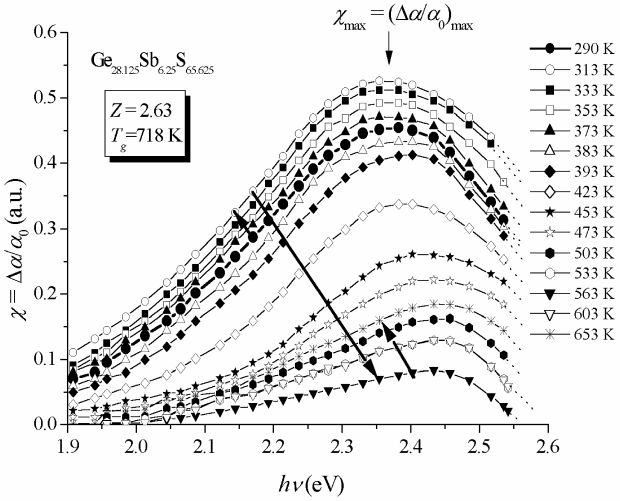

Fig. 1. Spectral dependences of γ-induced (Φ=3 MGy) darkening effect $\chi=(\Delta\alpha/\alpha_0)$ in v-$Ge_{28.125}Sb_{6.25}S_{65.625}$ (Z=2.63) after thermal annealing at different temperatures. The typical evolution of $\chi(h\nu)$ curves with thermal annealing temperature is shown by arrows.

3.1. As–Sb–S system

Fig. 2 shows the dependence of $\ln\chi_{max}$ versus $10^3/T_a$ for $As_{40}S_{60}$ and $As_{28}Sb_{12}S_{60}$ compositions (Z=2.40) of pseudobinary ("stoichiometric") As_2S_3-Sb_2S_3 cut-section of As–Sb–S system.

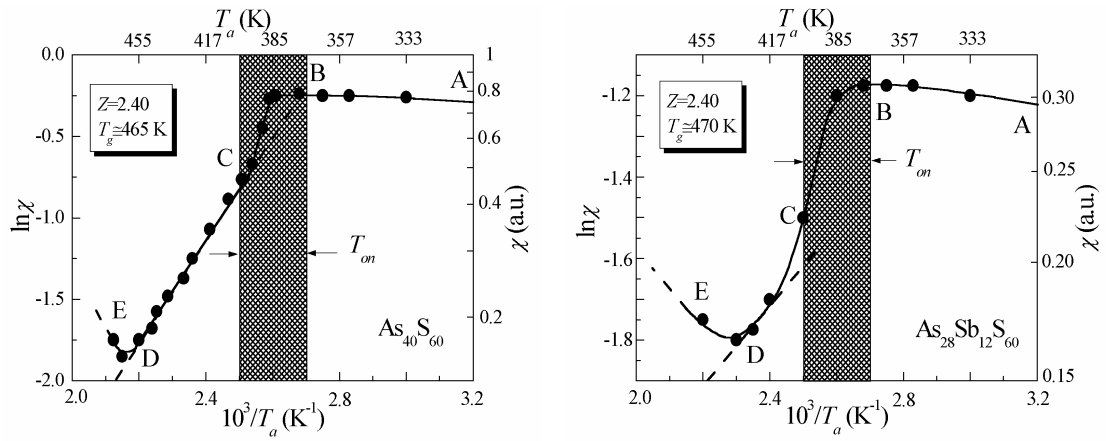

Fig. 2. Post-irradiation ($\Phi=10^7$ Gy) thermally-induced restoration determined by $\chi=(\Delta\alpha/\alpha_0)_{h\nu=2.10\ eV}$ parameter (the relative change of optical absorption coefficient α in the middle part of fundamental optical absorption edge region at $h\nu$=2.10 eV or λ=590 nm) versus thermal annealing temperature T_a for v-As_2S_3 (left) and v-$As_{28}Sb_{12}S_{60}$ (right). The bold lines through experimental points are drawn as a guide for the eye.

In the low-temperature region (AB) from room temperature T_A up to T_B, the slight increase in the post-irradiation RIOE with the apparent activation energies E_{AB}= 0.009 eV for v-As_2S_3 and E_{AB}= 0.011 eV for v-$As_{28}Sb_{12}S_{60}$ is observed.

In the threshold temperature region (BCD) from the onset temperature $T_B=T_{on}$ up to the maximal restoration temperature $T_D=T_{max}$, the strong restoration of the post-irradiation RIOE or post-irradiation ThSR effect takes place with apparent activation energies E_a=0.27±0.02 eV for v-As_2S_3 and E_a=0.10±0.02 eV for v-$As_{28}Sb_{12}S_{60}$. Because of the same anomalies in the vicinity of the onset temperatures (see in advance Figs. 4 and 6), the T_{on} values could be determined only approximately in crosshatched temperature range (Fig. 2). They are close to 370-400 K.

In the high-temperature region (DE) from $T_D=T_{max}$ up to $T_E<T_g$ the increase of the post-irradiation RIOE is observed for both v-As_2S_3 and for v-$As_{28}Sb_{12}S_{60}$.

3.2. Ge–As–S system

Figs. 3 and 4 show the dependence of $\ln\chi_{max}$ versus $10^3/T_a$ for ChG chemical compositions of pseudobinary 'stoichiometric' As_2S_3-GeS_2 and 'non-stoichiometric' As_2S_3-Ge_2S_3 cut-sections of Ge–As–S system.

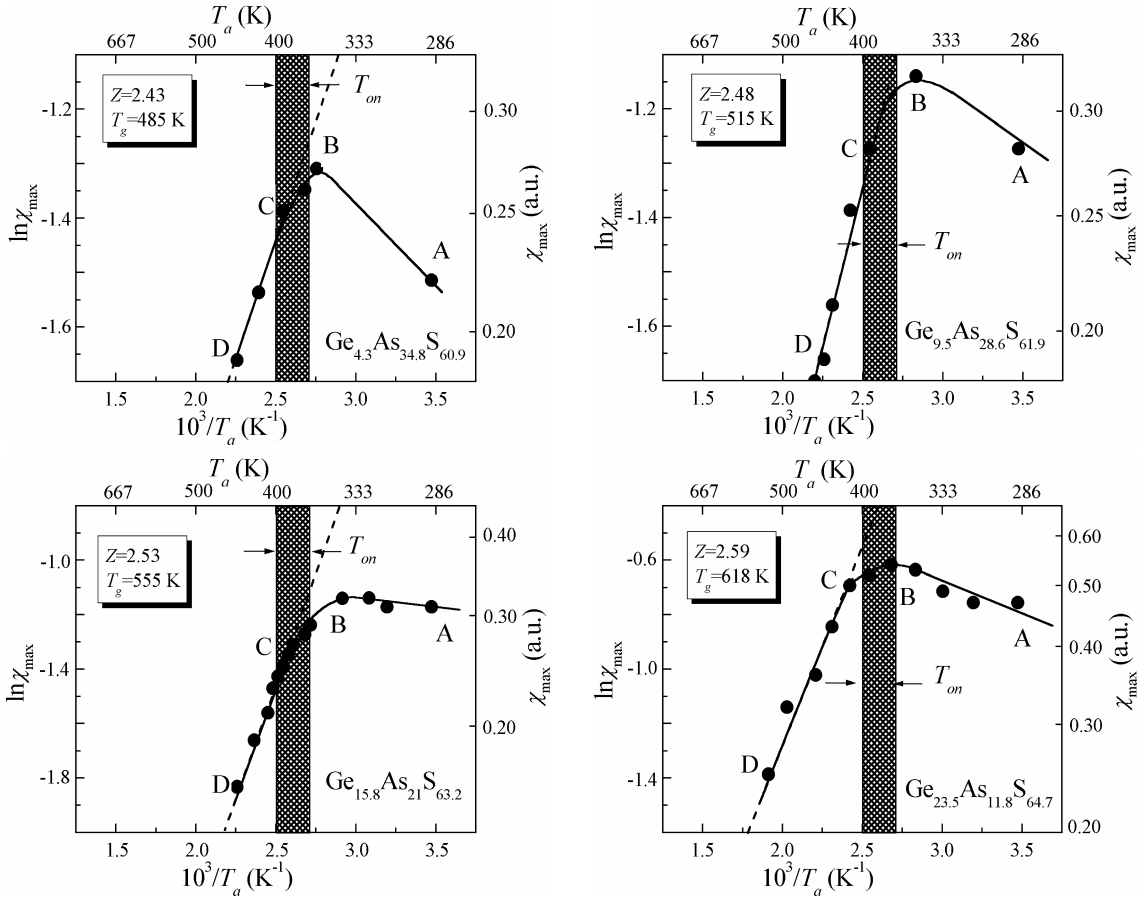

Fig. 3. Post-irradiation (Φ=2.2 MGy) thermally-induced restoration determined by $\chi_{max}=(\Delta\alpha/\alpha_0)_{max}$ parameter (the maximal value of the relative change of optical absorption coefficient α) versus thermal annealing temperature T_a for pseudobinary 'stoichiometric' v-As_2S_3–GeS_2: Z=2.43 (upper - left), Z = 2.48 (upper - right), Z=2.53 (lower-left) and Z=2.59 (lower-right). The bold lines through experimental points are drawn as a guide for the eye.

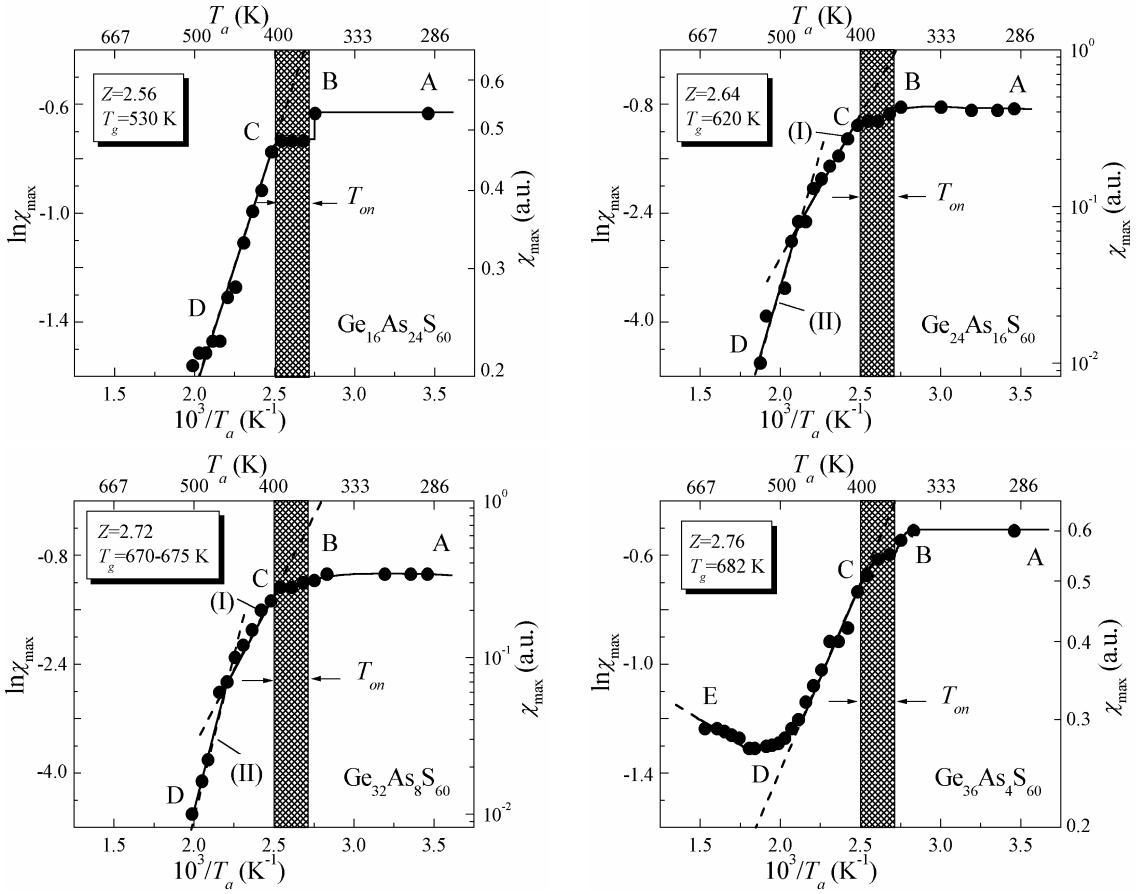

Fig. 4. Post-irradiation (Φ=4.4 MGy) thermally-induced restoration determined by $\chi_{max}=(\Delta\alpha/\alpha_0)_{max}$ parameter (the maximal value of the relative change of optical absorption coefficient α) versus thermal annealing temperature T_a for 'non-stoichiometric' v-As_2S_3–Ge_2S_3: Z=2.56 (upper-left), Z=2.64 (upper-right), Z=2.72 (lower-left) and Z=2.76 (lower - right). The bold lines through experimental points are drawn as a guide for the eye.

In the low-temperature region (AB) from T_A up to T_B, the increase of the post-irradiation RIOE with the character apparent activation energies E_{AB}= 0.026 eV @ Z=2.43, E_{AB}= 0.018 eV @ Z=2.48, E_{AB}= 0.006 eV @ Z=2.53 and E_{AB}= 0.021 eV @ Z=2.59 is observed for pseudobinary 'stoichiometric' ChG and the relative constancy in the post-irradiation RIOE ($E_{AB}\cong 0$) is obtained for all investigated glass compositions of 'non-stoichiometric' ones.

In the threshold temperature region (BCD) from $T_B=T_{on}$ up to $T_D=T_{max}$, the post-irradiation ThSR effect takes place with apparent activation energies E_a=0.07±0.02 eV @ Z=2.43, E_a=0.11±0.02 eV @ Z=2.48, E_a=0.12±0.02 eV @ Z=2.53 and E_a=0.13±0.02 eV @ Z=2.59 for pseudobinary 'stoichiometric' ChG and E_a=0.18±0.05 eV @ Z=2.56, E_a=0.51±0.05 eV @ Z=2.64, E_a=0.62±0.05 eV @ Z=2.72 and E_a=0.10±0.02 eV @ Z=2.76 for 'non-stoichiometric' one. Besides, in the case of 'non-stoichiometric' ChG, especially for glass composition with Z=2.56, the clear anomalies in the vicinity of the onset temperature (called as saddle regions) are revealed. The T_{on} values are typically close to 370-400 K.

In the high-temperature region (DE) from $T_D=T_{max}$ up to $T_E<T_g$, the increase of the post-irradiation RIOE is observed only for glass composition with highest Z value (Z=2.76) of 'non-stoichiometric' cut-section.

3.3. Ge–Sb–S system

Figs. 5 and 6 show the dependence of $\ln\chi_{max}$ versus $10^3/T_a$ for ChG chemical compositions of pseudobinary 'stoichiometric' Sb_2S_3-GeS_2 and 'non-stoichiometric' Sb_2S_3-Ge_2S_3 cut-sections of Ge–Sb–S system.

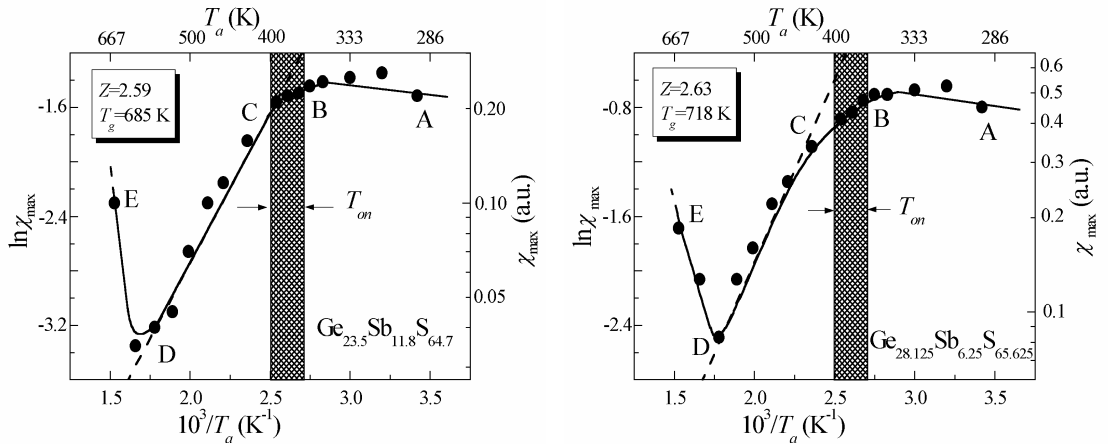

Fig. 5. Post-irradiation (Φ=3 MGy) thermally-induced restoration determined by $\chi_{max}=(\Delta\alpha/\alpha_0)_{max}$ parameter (the maximal value of the relative change of optical absorption coefficient α) versus thermal annealing temperature T_a for pseudobinary 'stoichiometric' v-Sb_2S_3–GeS_2: Z=2.59 (left) and Z = 2.63 (right). The bold lines through experimental points are drawn as a guide for the eye.

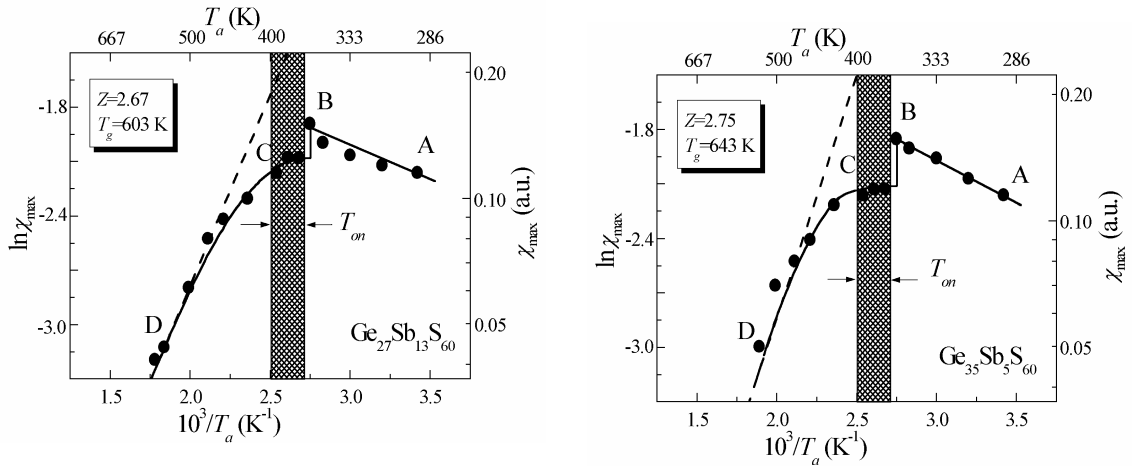

Fig. 6. Post-irradiation (Φ=3·10^6 Gy) thermally-induced restoration determined by $\chi_{max}=(\Delta\alpha/\alpha_0)_{max}$ parameter (the maximal value of the relative change of optical absorption coefficient α) versus thermal annealing temperature T_a for 'non-stoichiometric' v-Sb_2S_3–Ge_2S_3: Z=2.67 (left) and Z=2.75 (right). The bold lines through experimental points are drawn as a guide for the eye.

In the low-temperature region (AB) from T_A up to T_B, the increase of the post-irradiation RIOE with the character apparent activation energies E_{AB}= 0.013 eV @ Z=2.59 and E_{AB}= 0.015 eV @ Z=2.63 for pseudobinary 'stoichiometric' ChG and E_{AB}= 0.035 eV @ Z=2.67 and E_{AB}= 0.040 eV @ Z=2.75 for 'non-stoichiometric' one is observed.

In the threshold temperature region (BCD) from $T_B=T_{on}$ up to $T_D=T_{max}$, the post-irradiation ThSR effect takes place with apparent activation energies E_a=0.22±0.02 eV @ Z=2.59 and E_a=0.24±0.02 eV @ Z=2.63 for pseudobinary 'stoichiometric' ChG and E_a=0.20±0.02 eV @ Z=2.67

and Z=2.75 for non-stoichiometric one. It should be noted that for given ChG system, the anomalies in the vicinity of the onset temperature (called as saddle regions) are revealed some more clearly than that observed in the case of Ge–As–S one (see Figs. 4 and 6). The T_{on} values are also close to 370-400 K.

In the high-temperature region (DE) from T_D=T_{max} up to T_E<T_g, the increase of the post-irradiation RIOE is observed for glass compositions of pseudobinary 'stoichiometric' cut-section.

3.4. Summarizing of experimental data

The obtained experimental data are represented in Table 1 and can be summarized to the following. The post-irradiation ThSR effects are typically revealed in the investigated ChG (see Fig. 2, for example) through three regions in dependence on the thermal annealing temperature.

(1) *The low-temperature region* (AB) of the post-irradiation RIOE from room temperature T_A up to T_B which is observed as: (i) the slight increase in the post-irradiation RIOE with the character apparent activation energies E_{AB} of a few 0.01 eV (these energies are greater only in the ChG samples of 'non-stoichiometric' v-Sb_2S_3-Ge_2S_3 system reaching 0.40 eV); or (ii) the relative constancy of the post-irradiation RIOE (the character apparent activation energies E_{AB} are equal about zero as for v-As_2S_3-Ge_2S_3).

(2) *The threshold temperature region* (BCD) for strong restoration of the post-irradiation RIOE which is ranged from *the onset temperature* $T_B = T_{on}$ up to *the maximal restoration temperature* $T_D = T_{max}$. The some anomalies in the T_{on} vicinity (called the saddle regions) take place (see Fig. 4 for v-As_2S_3–Ge_2S_3 and Fig. 5 for v-Sb_2S_3–GeS_2). Sometimes, these saddle regions are revealed too slightly (see Fig. 2 for v-As_2S_3–Sb_2S_3 and Fig. 3 for v-As_2S_3–GeS_2) or more essentially in the form of break-off or jump regions (see Fig. 6 for v-Sb_2S_3–Ge_2S_3). Because of these anomalies the onset temperature T_{on} can be determined only approximately in the crosshatched temperature range in Figs. 2-6 and their values are typically close to 370-400 K independently on ChG composition. The maximal restoration temperature $T_D = T_{max}$ is the greatest temperature which can be used to restore maximally the post-irradiation RIOE without sample destroying. It can be seen from Table 1 that the greater T_g value for the investigated ChG leads to the greater maximal restoration temperature T_{max}. The quasi-linear temperature-dependent part with apparent activation energy E_a can be determined between the above onset T_{on} and maximal restoration T_{max} temperatures (the T_{on}-variation range is not included into consideration). The greater Z within 'stoichiometric' v-As_2S_3–GeS_2 ChG corresponds to the greater E_a value (see Table 1). Within 'non-stoichiometric' v-As_2S_3–Ge_2S_3 system, the E_a value demonstrates the sharply defined maximum near Z=2.7. Moreover, two quasi-linear parts with different but close activation energies can be distinguished within this temperature range for non-stoichiometric v-As_2S_3–Ge_2S_3 with Z close to 2.7 (see upper-right and lower-left curves in Fig. 4).

(3) *The high-temperature region* (DE) of the sharp increase in the post-irradiation RIOE at the thermal annealing temperatures close to T_g. This region is not observable in 'stoichiometric' v-As_2S_3– GeS_2 (see Fig. 3), while in 'non-stoichiometric' v-As_2S_3-Ge_2S_3 (see Fig. 4) it is strongly pronounced only at high Z values more than 2.7. On the contrary, in the ternary Ge–Sb–S system, this region is defined well in 'stoichiometric' v-Sb_2S_3–GeS_2 glasses (see Fig. 5), while it is negligible in 'non-stoichiometric' v-Sb_2S_3–Ge_2S_3 glasses even at high Z values (see Fig. 6).

4. Discussion

Two principally different kinds of structural defects are produced in the investigated ChG samples as result of γ-irradiation. The first one, *the nanoscale charged topological defects* in the form of over- (positively charged) and under-coordinated (negatively charged) atomic pairs caused by radiation-induced covalent bonds switching [7,14]. The second one, *the microscale inclusions* in the form of more or less pronounced phase-separated regions near the sample surface, containing not only own, but also impurity atoms (preferentially, oxygen, hydrogen, carbon and some of their chemical compounds, absorbed from atmosphere during radiation treatment) [7,15].

The first-kind defects are relatively stable to the annealing with temperatures less than T_{on}. Consequently, it can explain the observed independence of T_{on} (370-400 K) on ChG composition.

The increase of thermal annealing temperature leads to the threshold character of thermally-induced annihilation of these defects, showing a few anomalies in dependence on the defect type determined by the energetic balance of the corresponding radiation-induced switching reactions, the relationship between the number of hetero- and homopolar covalent chemical bonds in the nearest vicinity of charged atoms, the free-volume distribution around coordination defects, etc. [14,16]. From this position we can explain the observed compositional trends of apparent activation energy E_a in the investigated ChG. Namely, the formation of various radiation-induced defect types with different energies for their thermally-induced annihilation is supposed to give different E_a values. Therefore, the increasing of E_a with Z for pseudobinary 'stoichiometric' ChG and the greatest E_a values for glass compositions with Z close to 2.7 for 'non-stoichiometric' ChG can be interpreted by the formation in such glasses the most thermally stable radiation-induced defects. It is significant that the observed compositional trend of E_a well agrees with compositional behaviour of the free volume in these amorphous chalcogenides [17,18], which is favourable condition for stabilisation of the radiation-induced defects [19]. Apparently, this fact testifies to correspondence of above explanation regarding E_a compositional trends. Second confirmation can be also obtained taking into account the energetic balance of chemical bonds, which form the glassy network of the investigated ChG. In this case, the most energetic Ge–S bonds are mainly responsible for radiation-induced changes in ChG compositions with larger Z (Ge-enriched ChG) [17,18]. It means that the energies necessary for thermally-induced annihilation of defects connected with radiation-induced switching of Ge–S bonds should be greater in comparison with other coordination defect types. In such way, consequently, we can also explain the compositional features of E_a for ChG without Ge atoms, namely, for v-As–Sb–S system. Indeed, for v-$As_{40}S_{60}$ and v-$As_{28}Sb_{12}S_{60}$ from v-As_2S_3-Sb_2S_3, despite the similar Z values (Z=2.4) due to chemical substitution of three-coordinated As by three-coordinated Sb, the smaller E_a values for Sb-containing ChG can be interpreted in terms of well-known negative role of antimony in RIOE and formation of radiation-induced defects [17].

The second-kind defects, being produced by complex thermo-radiation influence (i.e. radiation-induced heating of the ChG), cannot be removed thermally. They reveal the temperature activated behaviour in the whole range of annealing temperatures with the following more essential expression near T_g, giving as a result: (i) the low-temperature region (AB) of the post-irradiation RIOE from room temperature T_A up to T_B, observed mainly as the slight increase of the post-irradiation RIOE with the apparent activation energies $E_{AB}\cong 0.01\div 0.02$ eV (the greater $E_{AB}\cong 0.35$-0.40 eV for v-Sb_2S_3-Ge_2S_3 could be explained by stronger low-temperature phase-separation processes); (ii) the high-temperature region (DE) of the sharp increase of the post-irradiation RIOE at T_a close to T_g, typical for some ChG, which can be connected with sharp increase of optical scattering of the irradiated samples. We suppose that such thermally stimulated scattering effect is well pronounced in non-stoichiometric v-As_2S_3-Ge_2S_3 at Z higher than 2.7 due to intensive high-temperature phase-separation processes. Certain confirmation for this assumption can be found in [20]. On the contrary, in the Ge–Sb–S ternary, the thermally stimulated scattering is well defined in 'stoichiometric' v-Sb_2S_3-GeS_2 glasses (see Fig. 5), based on bad glass-forming groups such as Sb_2S_3 and GeS_2. Deviations from stoichiometry due to additional homopolar chemical bonds within 'non-stoichiometric' v-Sb_2S_3–Ge_2S_3 system improve the overall ChG stability against the above high-temperature phase-separation processes.

In order to estimate the 'pure' contribution of the second-kind defects in the observed post-irradiation ThSR processes we have investigated ChG composition in which the contribution of the first-kind defects is negligible or radiation-induced changes of fundamental optical absorption edge are absent. From the studied ChG families, such characteristic is possessed to Sb-enriched 'non-stoichiometric' v-$Ge_{15}Sb_{25}S_{60}$ sample (Z=2.55), which normally does not reveal any observable RIOEs due to high metallization ability of Sb atoms [17]. The results of such probe experiment of T_a influence on the optical absorption spectrum of γ-irradiated (Φ=3 MGy) v-$Ge_{15}Sb_{25}S_{60}$ testify that E_{AB} value can reach even a more sufficient level (0.08 eV), following by sharp increase in optical

scattering due to thermally activated phase-separation processes, sufficiently enforced when the thermal annealing temperature T_a is close to T_g (see Fig. 7).

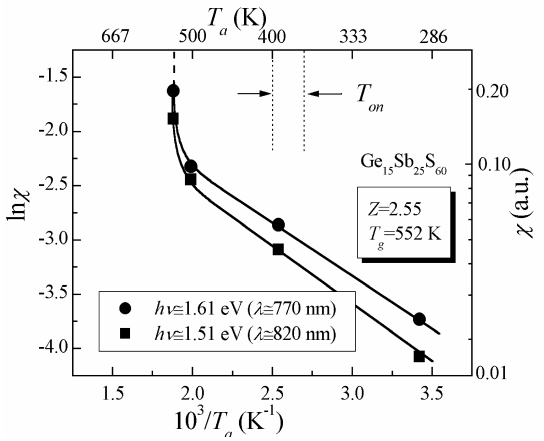

Fig. 7. The dependence of $\chi=\Delta\alpha/\alpha_0$ parameter (the relative γ-induced (Φ=3 MGy) change of optical absorption coefficient α) calculated at photon energies $h\nu$=1.51 eV or λ=770 nm and $h\nu$=1.61 eV or λ=820 nm in v-$Ge_{15}Sb_{25}S_{60}$ (Z=2.55) of 'non-stoichiometric' v-Sb_2S_3–Ge_2S_3 versus thermal annealing temperature T_a. The bold lines through experimental points are drawn as a guide for the eye.

5. Conclusions

The investigation of influence of thermal annealing temperature T_a on the optical absorption fundamental edge of preliminarily γ-irradiated As–Sb–S, Ge–As–S and Ge–Sb–S ternaries ChG from pseudobinary 'stoichiometric' and 'non-stoichiometric' cut-sections demonstrates that the established post-irradiation thermally stimulated restoration effects are typically revealed in these ChG through the following three regions in dependence on the thermal annealing temperature:

1) the low-temperature region of γ-induced optical effects beginning from room temperature up to the onset temperature T_{on} (where T_{on}≅370-400 K is independent on ChG composition);
2) the threshold temperature region of the strong restoration of γ-induced optical effects ranging from T_{on} up to the maximal restoration temperature T_{max} (where T_{max} is the greatest temperature, which can be used to restore maximally these post-irradiation optical effects without sample destroying);
3) the high-temperature region of the sharp increase of γ-induced optical effects beginning from T_{max} up to the thermal annealing temperature T_a closed to glass transition temperature T_g.

The compositional trends of the apparent activation energy E_a of the post-irradiation ThSR effects correlate well with compositional features of the free volume in the investigated ChG. The possible mechanisms of the observed phenomena can be considered in terms of the different kinds of structural defects, which can be produced in the investigated ChG samples as a result of γ-irradiation.

References

[1] J. S. Sanghera, I. D. Aggarwal, J. Non-Cryst. Solids **256-257**, 6 (1999).
[2] A. Saliminia, A. Villeneuve, T.V. Galstyan, S. LaRochelle, K. Richardson, J. Lightwave Technol., **17**, 837 (1999)
[3] J.-F. Viens, C. Meneghini, A. Villeneuve, T. V. Galstian, E. Knystautas, M. A. Duguay, K. A. Richardson, T. Cardinal, J. Lightwave Technol., **17**, 1184 (1999).
[4] O. I. Shpotyuk, A. P. Kovalskiy, J. Optoelectron. Adv. Mater. **4**, 751 (2002).
[5] K. Shimakawa, A. Kolobov, S. R. Elliot, Adv. Phys. **44**, 475 (1995).

[6] A. Ozols, O. Nordman, N. Nordman, J. Opt. Soc. Am. B **15**, 2355 (1998).
[7] O. I. Shpotyuk, A. O. Matkovskii, J. Non-Cryst. Solids **176**, 45 (1994).
[8] O. I. Shpotyuk, I. V. Savytsky, Ukr. Fiz. Zh. **34**, 894 (1989).
[9] M. F. Thorpe, J. Non-Cryst. Solids **57**, 355 (1983).
[10] H. Ticha, L. Tichy, N. Rysava, A. Triska, J. Non-Cryst. Solids **74**, 37 (1985).
[11] A. Feltz, Amorphe und Glasartige Anorganische Festkörper, Akademie-Verlag, Berlin (1983).
[12] V. Pamukchieva, E. Savova, M. Baeva, Phys. Chem. Glasses **36**, 328 (1998).
[13] S. Onari, T. Inokuma, H. Kataura, T. Arai, Phys. Rev. B **35**, 4373 (1987).
[14] O. I. Shpotyuk, R. Ya. Golovchak, A. P. Kovalskiy, V. Pamukchieva, E. Skordeva, D. Arsova, Ukr. J. Phys. Opt. **3**, 134 (2002).
[15] O. I. Shpotyuk, T. S. Kavetskyy, A. P. Kovalskiy, V. Pamukchieva, Proc. SPIE **4415**, 272 (2001).
[16] O. I. Shpotyuk, J. Filipecki, M. Hyla, A. P. Kovalskiy, R. Ya. Golovchak, Physica B **308-310**, 1011 (2001).
[17] O. I. Shpotyuk, T. S. Kavetskyy, A. P. Kovalskiy, Proc. SPIE **5122**, 95 (2003).
[18] A. Kovalskiy, J. Optoelectron. Adv. Mater. **3**, 323 (2001).
[19] E. A. Zhilinskaya, V. N. Lazukin, N. Kh. Valeev, A. K. Oblasov, J. Non-Cryst. Solids **124**, 48 (1990).
[20] P. Boolchand, D. G. Georgiev, T. Qu, F. Wang, L. Cai, S. Chakravarty, C. R. Acad. Sci. II C **5**, 1 (2002).